POWER SYSTEM FREQUENCY ESTIMATION ALGORITHM FOR ELECTRIC ENERGY METERING OF NONLINEAR LOADS

Zhang Peng, Li Hong-Bin

Huazhong University of Science and Technology, College of Electric and Electronic Engineering, Wuhan, China,
(✉ pzhill_108hust@yahoo.cn, +86 027 8754 8655, lihongbin@mail.hust.edu.cn, +86 027 8748 4147)

Abstract

In this paper, a discrete wavelet transform (DWT) based approach is proposed for power system frequency estimation. Unlike the existing frequency estimators mainly used for power system monitoring and control, the proposed approach is developed for fundamental frequency estimation in the field of energy metering of nonlinear loads. The characteristics of a nonlinear load is that the power signal is heavily distorted, composed of harmonics, inter-harmonics and corrupted by noise. The main idea is to predetermine a series of frequency points, and the mean value of two frequency points nearest to the power system frequency is accepted as the approximate solution. Firstly the input signal is modulated with a series of modulating signals, whose frequencies are those frequency points. Then the modulated signals are decomposed into individual frequency bands using DWT, and differences between the maximum and minimum wavelet coefficients in the lowest frequency band are calculated. Similarities among power system frequency and those frequency points are judged by the differences. Simulation results have proven high immunity to noise, harmonic and inter-harmonic interferences. The proposed method is applicable for real-time power system frequency estimation for electric energy measurement of nonlinear loads.

Keywords: frequency estimation, power systems, wavelet transforms.

1. Introduction

In recent years, the electric energy metering for nonlinear loads has drawn the attention of many researchers. For nonlinear loads, the total active power P can be described by (1), where fundamental active power P_1 and harmonic active power P_H are given by (2) and (3) respectively.

$$P = \frac{1}{T}\int_0^T u(t)i(t)dt = P_1 + P_H ,\qquad(1)$$

$$P_1 = V_1 I_1 \cos\theta_1 ,\qquad(2)$$

$$P_H = \sum_{h>1} V_h I_h \cos\theta_h .\qquad(3)$$

The standard IEEE1459-2000 [1] proposed that, for nonlinear loads, P_H and P_1 are separately metered, which helps to share power quality responsibility fairly between the consumer(s) and the electric power distributor [2].To measure P_1 and P_H, the fundamental frequency f_1 needs to be measured firstly. However, the voltage signal collected for frequency estimation is usually composed of harmonics, inter-harmonics, and dc offset, due to the impact of nonlinear loads [3-5]. Moreover, almost all electrical devices are virtually sources of electromagnetic interference. The voltage signal is unavoidably corrupted by noise during measurement and transmits periods. The paper [6] studied the intensity and behavior of noise

in low-voltage distribution systems. Therefore, for electric energy measurement of nonlinear loads, the frequency estimator should be able to estimate the fundamental frequency f_1 accurately when the input signal is heavily distorted by harmonics, inter-harmonics, noise etc. Take an energy meter of accuracy class 0.2 for example. The maximum error limit in energy registration is 0.2%, so the accuracy of fundamental frequency should be improved by two grades, i.e. class 0.05, and it means that the maximum allowable frequency error is 25 mHz for a 50 Hz power system.

In the past several decades, a variety of algorithms [7-26] for frequency estimation have been reported. Generally, the performance of a frequency estimation algorithm can be evaluated through static and dynamic tests. Static tests study the effects of harmonics or noise on the frequency estimator, and dynamic tests study the frequency-tracking performance. These existing algorithms are mainly used for power system monitoring, control and protection. When the power system frequency changes sharply, it will severely endanger the survival of a power system. Therefore these algorithms aim to track fast variations of frequency, and frequency tracking ability is more important than its accuracy and noise-immunity. However, in the fields of energy metering of nonlinear loads, accuracy and noise-immunity of the frequency estimator are especially emphasized, in addition to its frequency-tracking ability.

The modified zero-crossing method [7] and the modified Least Error Squares (LES) algorithm [8] have improved harmonic-resistant performance compared to their original versions. However, those methods still have somewhat poor noise performance. The Kalman filter-based technique includes the extended Kalman filter method [9], extended complex Kalman filter method [10] and robust complex Kalman filter [11]. Researchers try to improve the speed of convergence for frequency estimation, reduce the effects of the neglected high-order terms in Taylor's expansion, and enhance sensitivity and reliability for detecting a distorted signal. Those algorithms, including the discrete Fourier transforms method [12], transforming discrete Fourier transforms method [13], and Prony's method [14, 15], suffer from inaccuracies due to more violent fluctuations in the measured signal [11]. The paper [16] introduced an orthogonal FIR-filter-based frequency estimator, which has two averaging filters at the input and the output respectively. The input filter aims to reduce the effects of the 2nd-order and higher order harmonics. Similarly, the paper [17] studied an adaptive varying step-size Least Mean Square (LMS) method to improve immunity against noise disturbance. The proposed algorithm adopted a third-order Butterworth pre-filter with a crossover frequency of 200Hz to eliminate the effects of harmonics. For these algorithms in [16] and [17] it is a difficult task to design a filter to filter out the inter-harmonic component near to the fundamental frequency without degrading the algorithm's performance. The phase lock loop (PLL)-based method was proposed in [18] and compared with the adaptive notch filter (ANF)-based method in [19]. Comparison results show that the ANF-based method has better frequency-tracking performance; however, its harmonic (or noise) immunity is worse. In [20], the author introduced a least-squares method. The main characteristic of this algorithm is its short response time; however, its noise-immunity or harmonic-resistant ability is worse than that of the PLL-based method. The demodulation-based methods [21, 22] used two modulating signals. The signal components in the modulated signals, which carry the information of fundamental phase and also around DC, are filtered out by the low-pass filter and used for estimation of phase angle and frequency. The inter-harmonic component near the fundamental frequency, however, is still difficult to be filtered out. Other algorithms, such as the modified LMS algorithm [23], the least mean phase (LMP) algorithm [24] and the multi-harmonic least-squares fitting algorithm [25] are also reported. Reference [26] presents reviews of the existing several methods, outlining strengths and weaknesses of each one.

www.czasopisma.pan.pl   PAN   www.journals.pan.pl
POLSKA AKADEMIA NAUK

Metrol. Meas. Syst., Vol. XIX (2012), No. 2, pp. 307-320.

In power systems, the fundamental frequency usually deviates from its nominal value (50Hz or 60Hz), due to unbalance between generators and consumption or power fault [27, 28]. According to the standard EN50160 [29], the 10-second mean value of the fundamental frequency should be within 49.5–50.5 Hz during 99.5% of a year. Sergei S. Smirnov [30] pointed out that, according to European requirements [31], the average 10-minute frequency deviations should be within a ± 20 mHz range. And, based on field measurement, he reported that in Russia's power systems the fundamental frequency variation was in the range ±10 mHz and the maximum deviation amounts to ±50 mHz, with the averaging 10-minute period. Normally the rate of frequency variation was ±10 mHz/min (about $1.7e^{-4}$Hz/s) and may reach ±25mHz/min. (about $4.2e^{-4}$Hz/s). It can be observed from Figs [28, 32, 33] (Fig. 7 in [28], Fig. 6 in [32], Fig. 2.6 in [33]) that the rate of frequency fluctuation was normally about less than 20mHz/s under normal operating conditions. According to the above descriptions, the frequency estimator used in the field of power measurement of a nonlinear load should be able to track the slowly-changing frequency.

Wavelet transform is one of time-frequency techniques and has been applied in a wide variety of research areas such as transient analysis, harmonic analysis and power quality monitoring [34-38].Wavelets are oscillating waveforms with zero mean and start out at zero, increase and then decrease, which have zero amplitude at both ends. The basic idea underlying wavelet analysis involves expressing a section of a signal as a linear combination of a particular set of wavelet functions, and the coefficients represent how closely the wavelet function correlates with the signal in that section. These wavelet functions are obtained by shifting and dilating a mother wavelet. The discrete wavelet transform (DWT), as the digital representation of the continuous wavelet transform, decomposes a signal into different frequency components, and provides a logarithmic division of the frequency domain.

In this paper, the authors introduced a DWT-based approach to power frequency estimation. Similar with the methods [21, 22], the proposed method in this paper is also demodulation-based, using modulating signals ($sin(2\pi f_k t), cos(2\pi f_k t)$ and $sin(2\pi f_k t)+cos(2\pi f_k t)$). The difference between these two methods is that this approach is based on multi-level DWT. Estimation of fundamental frequency is achieved using wavelet coefficients in the lowest frequency band.

The multi-level DWT is implemented using a multistage filter bank with the wavelet function as the low-pass (LP) filter and its dual as the high-pass (HP) filter. Outputs of the LP filters are down-sampled by two for the next stage. To achieve Mallat's fast algorithm [34], the chosen mother wavelet should be orthogonal (or biorthogonal) and compactly supported. Among the commonly-used wavelets, wavelets that meet these requirements include Daubechies, Coiflets, Symlets and biorthogonal families. In comparison with a classical low-pass filter and a decimator that are used in most publications dealing with demodulation methods, the use of the discrete wavelet transform makes this algorithm show strong harmonic-resistance and noise-immunity. Here the 'harmonic' includes odd- and even-order harmonics, inter-harmonics, and sub-harmonics.

The paper is organized as follows. The concept of the proposed frequency estimator is explained in Section II. Section III evaluates the estimator performance under various conditions. Discussions about the proposed estimator are present in Section IV. Section V summarizes the main conclusions of the paper.

2. The proposed algorithm

In this section, the DWT-based algorithm for frequency estimation under nonlinear loads is introduced. The proposed frequency estimator employs *N* successive samples within a 0.2 second period (10 times the fundamental period for a 50 Hz system) to estimate the power

system frequency. Suppose the power signal (voltage signal or current signal) is band-limited such that a frequency component at or above 1500 Hz can be neglected. According to the Nyquist-Shannon sampling theorem, a 3200 Hz sampling frequency is chosen. The window size is 0.2 second, and the 640 successive samples within the window are decomposed by DWT at seven levels, and there are five wavelet coefficients in the lowest frequency band (0-12.5 Hz).

The main idea is as follows. Since the power system frequency f_1 usually fluctuates within a narrow frequency range (49.5 - 50.5 Hz for a 50 Hz power system) in normal operation, we can predetermine a series of frequency points within this interval, and find out the nearest frequency point (denoted as f_a) and the second nearest frequency point (denoted as f_b) to f_1 by some means. The mean value of f_a and f_b is considered as the approximate evaluation of f_1, i.e., $f_1 \approx 0.5(f_a+f_b)$. Two problems arise here. The first one is how to set up these frequency points. The second one is how to judge the similarity between these frequency points and f_1.

The first problem is easy to solve. When the proposed frequency estimator is initially started, eleven frequency points are 49.5 Hz, 49.6 Hz,…, 50.4 Hz and 50.5 Hz respectively, equally-spaced in the interval [49.5 Hz, 50.5 Hz]. In the following estimation, the interval is limited within the neighborhood of the previous estimated frequency (denoted as f_x), i.e., [f_x-0.05 Hz, f_x+0.05 Hz]. Choice of 0.05Hz is based on the following considerations. In the first estimation, the interval between adjacent frequency points is 0.1 Hz. Assume the actual fundamental frequency is between the frequency points 49.9 Hz and 50.0 Hz, and the estimated frequency will be 49.95 Hz. The difference between the actual frequency and its estimated value is less than 0.05 Hz. The modified frequency range is obviously narrower than the initial range and the interval between adjacent frequency points is decreased to 0.01 Hz ((f_x+0.05 Hz)-(f_x-0.05 Hz)/10=0.01 Hz). This fact helps to increase estimation accuracy. Meanwhile, modification of the frequency range realizes the frequency-tracking capability when the power system frequency fluctuates.

The second problem is exactly how to find out the frequency points f_a and f_b from these frequency points. A detailed approach is as follows: use these predetermined frequency points as the frequencies of a series of modulating signals, and the power signal is modulated by these modulating signals. Those frequency components in the modulated signals whose frequencies equal the difference between the power system frequency f_1 and these frequency points, are separated out using DWT, and the corresponding wavelet coefficients are obtained. Denote the difference between the maximum and minimum coefficients in the lowest frequency band as D_f. For each modulated signal, one corresponding D_f value is obtained. The frequency point corresponding to the minimum D_f value is considered as the frequency point nearest to f_1, .i.e., f_a.

Assume the power signal $v(t)$ is represented by :

$$v(t) = V_1 \sin(2\pi f_1 t + \theta_1) + \sum_{k=2}^{M} V_k \sin(2\pi f_k t + \theta_k). \tag{4}$$

Here f_1, V_1 and θ_1 (or f_k, V_k and θ_k) represent the frequency, amplitude and initial phase angle of the fundamental component (or the hth harmonic component) respectively. f_k equals kf_1, and M is the highest harmonic order. Generate a modulating signal $a_m(t)$, defined by (5). The frequency f_m is selected from these frequency points.

$$a_m(t) = \sin(2\pi f_m t). \tag{5}$$

Multiply $v(t)$ by $a_m(t)$, the modulated signal $v_a(t)$ is obtained:

$$v_a(t) = v(t)a_m(t) = \sum_{k=1}^{M} V_k \sin(2\pi f_k t + \theta_k)\sin(2\pi f_m t), \tag{6}$$

www.czasopisma.pan.pl   PAN   www.journals.pan.pl
POLSKA AKADEMIA NAUK

Metrol. Meas. Syst., Vol. XIX (2012), No. 2, pp. 307-320.

where

$$\sin(2\pi f_k t + \theta_k)\sin(2\pi f_m t)$$
$$= \frac{1}{2}\cos[2\pi(f_k - f_m)t + \theta_k] - \frac{1}{2}\cos[2\pi(f_k + f_m)t + \theta_k]. \tag{7}$$

It can be seen from (7) that the frequency components in the signal $v_a(t)$ can be represented as $(f_k - f_m)$ or $(f_k + f_m)$, and k varies from one to M. Usually f_1 is in the frequency range of 49.5 to 50.5 Hz, and f_m also belongs to this range, so the lowest frequency component is $\Delta f_1 (=|f_1 - f_m|)$, $\Delta f_1 \in [0\ \text{Hz}, 1\ \text{Hz}]$.

Using multi-level DWT, $v_a(t)$ is decomposed into wavelet coefficients of individual frequency bands. The lowest frequency band is $(0 - W_b)$ Hz, and W_b is denoted as the frequency band width. To separate out the frequency component Δf_1, W_b should be less than 50Hz when $v_a(t)$ is only composed of a fundamental component and integer harmonics. However, if inter-harmonics exist in $v(t)$, frequency component $|f_{inter} - f_m|$ in the signal $v_a(t)$ may be less than 25 Hz. Here f_{inter} is the inter-harmonic frequency. In such case, W_b should be further decreased in order to separate out Δf_1. In the following evaluation section, W_b is 12.5 Hz.

After obtaining the wavelet coefficients, D_f is calculated. Using eleven different frequency points as the frequency f_m respectively, eleven Δf_1 and the corresponding eleven D_f values are obtained.

Apart from signal $a_m(t)$, two different modulating signals $b_m(t)$ and $c_m(t)$ are also studied, given by (8) and (9).

$$b_m(t) = \cos(2\pi f_m t). \tag{8}$$

$$c_m(t) = a_m(t) + b_m(t). \tag{9}$$

Studies show that D_f has a certain relationship with Δf_1, when Δf_1 belongs to the interval [0 Hz, 1 Hz]. When the initial phase angle θ_1 belongs to a certain interval (discussion below), D_f monotonically grows with the increase in Δf_1. This interval is called a monotone interval, or in other words, the corresponding modulating signal is considered to be monotonic in this interval. Fig. 1(a) shows the monotone and non-monotone intervals corresponding to the modulating signals $a_m(t)$, $b_m(t)$ and $c_m(t)$ respectively. It is observed that there are always two or more modulating signals that are monotonic when θ_1 varies from 0 degrees to 360 degrees with a step of 1 degree, except several narrow intervals. In the monotone interval, the frequency point corresponding to the minimum D_f is nearest to f_1 among all frequency points.

However, when the initial phase angle θ_1 values are in those intervals ([43-Δ,43+Δ], [178-Δ,178+Δ], [223-Δ,223+Δ], [358-Δ,358+Δ],0<Δ<1, unit (degrees)), only one modulating signal is monotonic. Further research shows that, for those intervals, although in the whole interval [0 Hz, 1 Hz] of Δf_1 a certain modulating signal is not monotonic, there is still a narrower interval in which the signal is monotonic. Furthermore, the D_f value corresponding to the minimum Δf_1 is also the minimum. For example, when the initial angle θ_1 is 358 degrees, the relationship of D_f values versus Δf_1 is depicted in Fig. 1(b). Here the signal $a_m(t)$ is monotonic for the whole interval [0 Hz, 1 Hz], and the non-monotonic intervals for signals $b_m(t)$ and $c_m(t)$ are [0.04 Hz, 0.05 Hz] and [0.99 Hz, 1 Hz] respectively. So two or more modulating signals are monotonic whatever the frequency deviation is, when the initial phase angle θ_1 is 358 degrees.
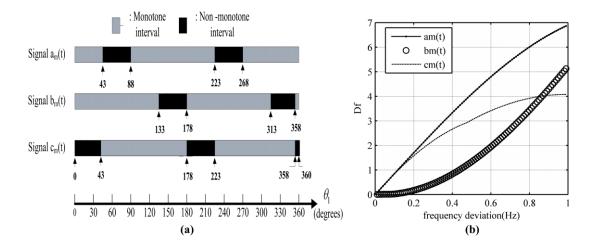
Fig. 1. (a) Monotone and non-monotone intervals for the modulating signal $a_m(t)$, $b_m(t)$ and $c_m(t)$
(b) Relationship of D_f value versus frequency deviation Δf_1 when θ_1 is 358 degrees.

Synthesized from the above descriptions, the following conclusions are obtained. If two or more modulating signals determine the same points nearest to the fundamental frequency f_1, it means that this frequency point is f_a. Meanwhile, these corresponding modulating signals are monotonic.

After the point f_a is detected, the next step is to find out the second-nearest frequency point f_b. There are two frequency points nearest to f_a among all frequency points, one on the left side (denoted as f_{b1}) and the other on the right side (denoted as f_{b2}). When the modulating signal is in the monotone interval, the frequency point corresponding to the smaller D_f value is f_b. For example, if the frequency point f_a is 49.7 Hz, co-determined by the signals $a_m(t)$ and $b_m(t)$, the two frequency points nearest to f_a are 49.6 Hz and 49.8 Hz respectively. According to the fore-mentioned description, the signals $a_m(t)$ and $b_m(t)$ are both in the monotone interval. Select one of the two signals arbitrarily, for example, $a_m(t)$. For signal $a_m(t)$, if the D_f value of the right point (49.8 Hz) is smaller than that of the left point (49.6 Hz), f_b is 49.8 Hz.

According to the linearity of discrete wavelet transform [39, 40], (10) exits, where $DWT(\cdot)$ means the discrete wavelet transform operator. Equation (10) shows that the wavelet coefficients of signal $c_m(t)$ can be directly calculated from those of signals $a_m(t)$ and $b_m(t)$, and therefore calculation complexity is reduced.

$$DWT(c_m(t)) = DWT(a_m(t)) + DWT(b_m(t)) . \qquad (10)$$

3. Evaluation of the proposed algorithm

The performance of the DWT-based frequency estimator proposed in this paper has been evaluated under static and dynamic conditions using computer simulation. In the static tests, the effects of noise, harmonics, inter-harmonics and dc offset are evaluated. In the dynamic tests, the capability of the frequency estimator in tracking step, ramp, and oscillatory variations of frequency is evaluated. Effects of amplitude and phase jumps in the power signal are also studied. The evaluation is compared with the PLL-based method [18] and the ANF-based method [19]. Finally the voltage samples collected from the power system are analyzed by the proposed algorithm. Here the sampling frequency is 3200 Hz, the wavelet function is db5, and the window size is 0.2 second (640 samples). Seven-level DWT is performed to obtain the wavelet coefficients in the frequency band (0-12.5 Hz). Similar results are obtained when other wavelet functions (wavelets that belong to Daubechies, or Coiflets, or Symlets or biorthogonal families) are used, and are not shown here for simplification.

www.czasopisma.pan.pl PAN www.journals.pan.pl
POLSKA AKADEMIA NAUK

Metrol. Meas. Syst., Vol. XIX (2012), No. 2, pp. 307-320.

3.1. Static test

3.1.1. Noise

The test signal is a pure sinusoidal signal with unity amplitude, corrupted with zero-mean Gaussian white noise. Fig. 2 (a) shows maximum errors of the proposed algorithm, the ANF-based method and the PLL-based method, when the sinal-to-noise ratio (SNR) varies from 20dB to 60dB. It is observed that the noise immunity feature of the proposed algorithm is desirable, and competes with that of the ANF-based method. However, the proposed frequency estimator provides less-accurate responses compared with the PLL-method, when noise is present.

3.1.2. Harmonics and DC Component

To study the impact of harmonics and DC offset on the performance of the frequency estimator, several examples are considered, where the input signal is a fundamental component plus dc offset, or a fundamental component plus a third harmonic, or a fundamental component plus a fifth harmonic, or composed of a fundamental component, dc offset and harmonics ($2^{nd} \sim 25^{th}$). The estimated frequency has a fixed error (5 mHz) when the relative magnitude of dc offset or a single harmonic component with respect to that of the fundamental component varies from 0% to 50%. This study shows that the impact of dc offset or harmonics is negligible. For the ANF-based method or the PLL-based method, the estimated frequency is subject to an oscillatory steady-state error and an offset error. The maximum error equals the sum of the oscillatory and offset errors due to individual harmonic components. For example, when the test signal is composed of a fundamental and the 3rd harmonic component, the maximum errors of these frequency estimators are illustrated in Fig. 2 (b).

It is observed that the performance of the proposed algorithm is better, compared with the ANF based method. In the case of low harmonic distortion level, the performance of the PLL-based method competes with the proposed method. However, when the harmonic distortion level increases, the proposed method outperforms the PLL-based method. Meanwhile, the PLL-based method uses a second-order band-pass pre-filter to reduce the effects of harmonics, and the cutoff frequencies are 10 Hz and 110 Hz. Obviously, an inter-harmonic frequency component near to the fundamental frequency is difficult to be filtered off by this filter. And the task to design such a filter without degrading the performance of the frequency estimator is difficult to achieve.

3.1.3. Inter-harmonics

The test signal is composed of a fundamental component with unity amplitude and an inter-harmonic component. Three cases with different inter-harmonic amplitude (0.01 p.u, 0.02 p.u, and 0.05 p.u) are studied. When the inter-harmonic frequency varies from 15 Hz to 48 Hz, the maximum estimation error of the proposed estimator is depicted in Fig. 2 (c). It is observed that the estimation error depends on the inter-harmonic frequency and amplitude. For example, when the input signal is composed of a fundamental component and the inter-harmonic component (frequency: 40 Hz, amplitude: 0.05), the error is less than 35 mHz. This study shows that the proposed algorithm has a strong inter-harmonic immunity.
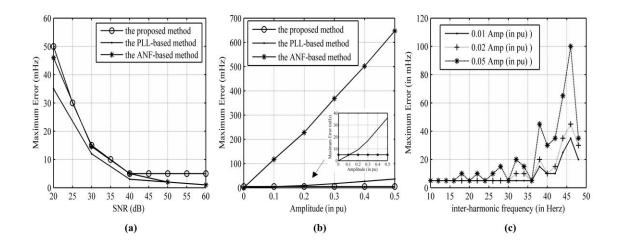
Fig. 2. Impact of (a) noise (b) harmonics (c) inter-harmonics on the estimated frequency.

3.2. Dynamic test

3.2.1. Jumps in Amplitude or Phase Angle

Switching may cause a step change in voltage amplitude or phase in power systems [41]. The impact of such step changes on the performance of the frequency estimator should be as small as possible. Simulation results show that step changes in the amplitude or phase angle result in no steady-state errors in the estimated frequency when the amplitude or phase of the input signal undergoes a jump of 0.5 pu (amplitude) or 60 degrees (phase). However, a transient error of 50 mHz is observed when the phase angle of the input signal jumps. For the PLL-based method or ANF-based method, step changes in the amplitude or phase angle also result in no steady-state errors in the estimated frequency. For the ANF-based method, the transient error is 200 mHz for an amplitude step, and 3 Hz for a phase angle step. For the ANF-based method, the transient error is 800 mHz for an amplitude step, and 1.5 Hz for a phase angle step. The drawback of the proposed frequency estimator is that its transient time is 0.2 second, longer than that of the PLL-based method (about 0.1s) or that of the ANF-based method (about 0.08s).

3.2.2. Oscillatory Variations of Amplitude

The impact of oscillatory variations of amplitude on the estimated frequency is studied. When the amplitude of the input signal changes from its nominal value of 1 to $1+0.2sin\pi t$, the maximum error of the estimated frequency is 5 mHz, less than 20 mHz of the ANF-based method.

The following section is devoted to verify the performance of the proposed frequency estimator in tracking various types of frequency variations, including ramp, step and oscillation. However, the proposed frequency estimator is used for a power energy meter. Therefore, different from those in [18] and [19], only frequency variations whose frequency-rate-of-change (df/dt) is less than 0.2 Hz/second or a single step-change is less than 0.2 Hz, are studied.

3.2.3. Ramp Variations of Frequency

The capability of the proposed method in tracking ramp variations of frequency is depicted in Fig. 3. The frequency-rate-of-change of the input signal is 0.1Hz/second. The true frequency and its estimated value are shown in Fig. 3(a), and the estimation error is shown in Fig. 3(b). This study shows that the estimated frequency faithfully follows the true ramp with a delay of 0.2 seconds.
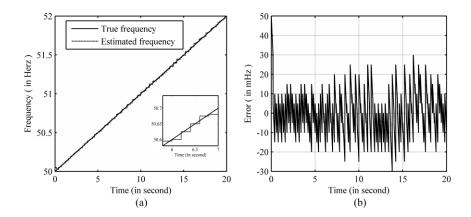

Fig. 3. Frequency tracking for ramp variation (a) frequency variation curves (b) the estimation error.

3.2.3. Oscillatory Variations of Frequency

The paper [41] pointed out that the power system frequency can fluctuate due to electromechanical oscillations of generators. An example is considered to illustrate the performance of the proposed estimator with respect to oscillatory frequency variations. The frequency of the input signal is $f (=50+sin0.04\pi t)$. The maximum rate of change of frequency is 0.04πHz/s(<0.2Hz/s). The actual frequency and its value estimated by the proposed estimator are shown in Fig. 4(a). It is observed that the estimated frequency follows the actual frequency with a delay of 200ms. Fig. 4(b) shows the estimation error. This study shows that the proposed frequency estimator can track frequency oscillatory variations when the rate of change of frequency is small.
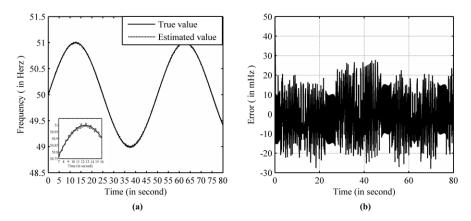

Fig. 4. Frequency tracking for oscillatory variation (a) frequency variation curves (b) the estimation error.

3.2.4. Step Variations of Frequency

Here the frequency of the input signal makes a step change at 2.7174 s. The actual frequency and its estimated values by the proposed estimator are shown in Fig. 5. Three cases with different step changes of 50 mHz, 100 mHz and 200 mHz are considered, and the corresponding results are illustrated in Fig. 5 (a),(b), and (c) respectively. It is observed that the steady-state error is 10 mHz no matter whatever the step change is; however, the transient time grows with an increase of the step change. It is so because the modification of the frequency estimation range takes more much time for a large step change. The response time of the proposed method is less than 600 ms for a step change of 50 mHz (or 100 mHz), and less than 1000ms for a step change of 200 mHz.

3.3. Frequency estimation using a real voltage signal from the power system

The voltage signal from the power system is adjusted by a voltage adjustor, and then through a converter (100V/4V), is finally collected by a NI6221 data acquisition card (National Instrument, 16-bit A/D converter). The collected signals are analyzed by the proposed algorithm, and the fluctuation curve of power system frequency is illustrated in Fig. 6. As the true frequency of the power system was not known, estimation errors cannot be calculated. However, the estimation quality of the proposed algorithm can be judged from their consistency [13, 16]. The maximum variation in the measured frequency is about ± 0.04Hz. This demonstrates the effectiveness of the proposed algorithm for power system frequency estimation.
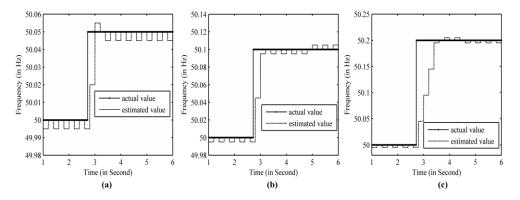

Fig. 5. Frequency tracking for step variations (a) 0.05 Hz step change (b) 0.1 Hz step change
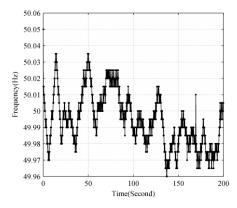(c) 0.2 Hz step change.

Fig. 6. Frequency measurement results of a voltage signal taken from the grid.

www.czasopisma.pan.pl   **PAN**   www.journals.pan.pl

POLSKA AKADEMIA NAUK

Metrol. Meas. Syst., Vol. XIX (2012), No. 2, pp. 307-320.

4. Discussions

The proposed estimator employs N successive samples within 10 times the nominal fundamental period (0.2 second for a 50 Hz power system). These samples are decomposed by multi-level DWT to obtain the wavelet coefficients in the lowest frequency band which are used to estimate the power system frequency. N equals $0.2f_s$, and f_s is the sampling frequency. Here some important parameters, including window size, decomposition level, sampling frequency and choice of wavelet function are needed to be further explained.

The sampling frequency f_s is selected to be 2^r times the nominal fundamental frequency and r is an integer. Also f_s should be higher than two times the harmonic frequency to meet the requirements of the Nyquist-Shannon sampling theorem. Usually frequency components higher than 1600 Hz are negligible, so the sampling frequency of 3200 Hz is an appropriate choice.

Here the choice of window size is based on the following considerations, in addition to the requirements of the standard [42]. If the window size is 5 times the nominal fundamental period, N equals $0.1f_s$. For multi-level DWT decomposition, assume the decomposition level is h, the number of wavelet coefficients (denoted as M) in the lowest frequency band will be $N/(2^h)$, and M should be an integer. When N equals $0.1f_s$, the maximum decomposition level is 5 (f_s=1600 Hz) or 6 (f_s=3200 Hz), and the lowest frequency band is (0 Hz-25 Hz). When N equals 0.2s, the maximum decomposition level is 6 (f_s=1600 Hz) or 7 (f_s =3200 Hz), and the corresponding lowest frequency band is (0 Hz-12.5 Hz), W_b is 12.5 Hz. As described in section II, the decrease of the lowest frequency bandwidth will help reduce the effects of inter-harmonics. So the window size is usually set to be 0.2s (for a 50 Hz system). According to the characteristics of multi-level DWT, the decomposition level (denoted as K) is decided by f_s and w_b, as described in (11). Here w_b is the width of the frequency band, which usually is selected to 12.5 Hz.

$$K = \log_2(\frac{f_s}{2w_b}).$$ (11)

For real-time power metering, the calculation procedure including estimation of the fundamental frequency, harmonic parameters, and calculation of power-related quantities should be done within a 0.2 s period. To simplify verification, the proposed algorithm is initially performed in the MATLAB environment and two commands (tic and tic) are used to make a rough estimation of execution time. It has been found that the execution time increases when the sample number increases or the number of wavelet filter coefficients (denoted as N_f) increases. Take the Daubechies family for example. N_f is 10 for Db5, or 20 for Db10, or 40 for Db20. Table 1 demonstrates different execution time when sample number or Db wavelet is different. Only three different wavelet functions (Db5, Db10 and Db20) are present in the table. Here the used computer is HP 540 (CPU: Intel(R) Core(TM) Duo CPU T 5670@ 1.80 GHz, 1.99 GHz). For example, if the sample time is 640 and the Db5 (or Db10) wavelet is used, the corresponding computation time is 97 (or 99) milliseconds. It means that Db5 or Db10 is suitable for real-time application. For further evaluation of computational complexity, implementation of the use of assembly language in the industry control computer will be the future research goal. Furthermore, theoretical analysis of the relationship between D_f and $\varDelta f_1$ will also be the further work, because it will be helpful to clarify the characteristics of this approach.

Table 1. Execution time of the proposed algorithm (in milliseconds).

Wavelet function	Sample number		
	320	640	1280
Db 5	59	97	211
Db10	60	99	214
Db20	281	398	679

5. Conclusions

This paper proposes a DWT-based approach for estimation of power system frequency. The noise immunity of this approach is comparable to that of the ANF-based method, and smaller than that of the ANF-based method. And its harmonic (or inter-harmonic) immunity outperforms those of PLL-based or ANF-based methods. The main drawback is the high computation complexity and the corresponding long computation time. Therefore, the dynamic response of the proposed method with regard to step, ramp, and oscillatory changes of frequency are slower than those of PLL-based or ANF-based methods. Simulation results show that the frequency error of the proposed algorithm is less than 25 mHz in most cases. Furthermore, if the proposed algorithm is implemented in parallel computation, the computation time will be greatly reduced. This approach is suitable for power system frequency estimation for energy metering of a nonlinear load.

Acknowledgements

References

[1]   IEEE Std. 1459-2000. (2000). Definitions for the Measurement of Electric Quantities Under Sinusoidal, Non-sinusoidal, Balanced, or Unbalanced Conditions. The Institute of Electrical and Electronics Engineers, Inc., New York.

[2]   Svensson, S. (1999). Power measurement techniques for non-sinusoidal conditions. *PhD thesis.* Chalmers University, Sweden.

[3]   IEEE Task Force on Harmonics Modeling and Simulation (2007). Inter-harmonics: Theory and Modeling. *IEEE Trans. Power Del.*, 22(4), 2335-2348.

[4]   Bellido, R.C., Gomez, T. (1997). Identification and modeling of a three phase arc furnace for voltage disturbance simulation. *IEEE Trans. Power Del.*, 12(4), 1812-1817.

[5]   Ribeiro, P.F. (2009). *Time-Varying Waveform Distortions in Power Systems*. Wiley-IEEE Press.

[6]   Ashton, P.T., Swift, G.W. (1990). Measurements of transient electrical noise on low voltage distribution systems. In *Proc. IEEE Ind. Appl. Soc. Annu. Meeting*, 1740-1742.

[7]   Miroslav, M.B , Petar, M.D., Dunlap, S., Arun, G.P. (1993). Frequency Tracking in Power Networks in the Presence of Harmonics. *IEEE Trans. Power Del.*, 8(2), 480-486.

[8]   Giray, M.M., Sachdev, M.S. (1989). Off-nominal frequency measurements in electric power systems. *IEEE Trans. Power Del.*, 4(3), 1573-1578.

[9]   Girgis, A.A., Peterson, W.L. (1990). Adaptive Estimation of Power Frequency Deviation and Its Rate of Change for Calculating Sudden Power System Overloads. *IEEE Trans. Power Del.*, 5(2), 585-593.

[10] Dash, P.K., Jena, R.K., Panda, G., Routray, A. (2000). An Extended Complex Kalman Filter for Frequency Measurement of Distorted Signals. *IEEE Trans. Instrum. Meas*, 49(4), 746-753.

[11] Huang, C.-H., Lee, C.-H., Shih, K.-J., Wang, Y.-J. (2010). A Robust Technique for Frequency Estimation of Distorted Signals in Power Systems. *IEEE Trans. Instrum. Meas.*, 59(8), 2026-2036.

[12] Phadke, A.G., Throp, J.S., Adamiak, M. (1983). A new measurement technique for tracking voltage phasors, local system frequency, and rate of change of frequency. *IEEE Trans. Power App. Syst.*, PAS-102(5), 1025-1038.

[13] Yang, R., Xue, H. (2008). A novel Algorithm for Accurate Frequency Measurement using Transformed Consecutive Points of DFT. *IEEE Trans. Power Syst.*, 23(3), 1057-1062.

[14] Lobos, T., Rezmer, J. (1997). Real-time determination of power system frequency. *IEEE Trans. Instrum. Meas.*, 46(4), 877-881.

[15] Zygarlicki, J., Mroczka, J. (2012). Variable-frequency Prony method in the analysis of electrical power quality. *Metrol. Meas. Syst.*, 19(1), 39-49.

[16] Szafran, J., Rebizant, W. (1998). Power system frequency estimation. *IEE proc.-Gener.Transm. Distrib.*, 145(5), 578-582.

[17] Pradhan, A.K., Routray, A., Basak, A. (2005). Power System Frequency Estimation Using Least Mean Square Technique. *IEEE Trans. Power Deliv.*, 20(3), 1812-1816.

[18] Houshang, K., Masoud, K.-G., et al. (2004). Estimation of Frequency and its Rate of Change for Applications in Power Systems. *IEEE Trans. Power Deliv.*, 19(2), 472-480.

[19] Mohsen, M., Masoud, K.-G., Alireza, B. (2007). Estimation of Power System Frequency Using an Adaptive Notch Filter. *IEEE Trans. Power Deliv.*, 56(6), 2470-2477.

[20] Ali, A., Farhad, M. (2011). Frequency Estimation: A Least-Squares New Approach. *IEEE Trans. Power Deliv.*, 26(2), 790-798.

[21] Djuric, P.M., Begovic, M.M., Doroslovacki, M. (1992). Instantaneous Phase Tracking in Power Networks by Demodulation. *IEEE Trans. Instrum. Meas*, 41(6), 963-967.

[22] D'Apuzzo, M., D'Arco, M. (2008). A Time-Domain Approach for the Analysis of Nonstationary Signals in Power Systems. *IEEE Trans. Instrum. Meas*, 57(9), 1969-1977.

[23] Barbosa, D., Monaro, R.M., Coury, D.V., Oleskovicz, M. (2010). Digital frequency relaying based on the modified least mean square method. *Int. J. Electr. Power Energ. Syst.*, 32(11), 236-242.

[24] Rawat, T.K., Parthasarathy, H., Oleskovicz, M. (2008). A continuous-time least mean-phase adaptive filter for power system. *Int. J. Electr. Power Energ. Syst.*, DOI:10.1016/j.ijepes.2008.10.012

[25] Ardeleanu, A.S., Ramos, P.M. (2011). Real time PC implementation of power quality monitoring system based on multiharmonic least-squares fitting. *Metrol. Meas. Syst.*, 18(4), 543-554.

[26] Ramos, P.M., Cruz Serra, A. (2009). Comparison of frequency estimation algorithms for power quality assessment. *Measurement*, 42, 1312-1317.

[27] Bollen, M.H.J., Yu-Hua Gu, I. (2006). *Signal Processing of Power Quality Disturbances*. IEEE Press, John Wiley & Sons, Inc.

[28] Kirby, B.J., Dyer, J., Martinez, C., Shoureshi, R.A., Guttromson, R., Dagle, J. Frequency Control Concerns In The North American Electric Power System. *www.ornl.gov/~webworks/cppr/y2001/rpt/116362.pdf.*

[29] EN50160 (2007).Voltage characteristics of electricity supplied by public distribution systems.

[30] Smirnov, S.S. Measurement Results of Frequency and Exchange Power Fluctuations in Russia's Power System. *www.sei.irk.ru/files/publication/24.pdf.*

[31] Union for the Co-ordination of Transmission of Electricity: Operation Handbook. (2004). Brussels. *http://www.ucte.org.*

[32] Giæver Tande, J.O. (2002). Applying Power Quality Characteristics of Wind Turbines for Assessing Impact on Voltage Quality. *SINTEF Energy Research*, 5, 37-52.

[33] Zhong, Z. (2005). Power Systems Frequency Dynamic Monitoring System Design and Applications. *PhD*

thesis. Virginia Polytechnic Institute and State University.

[34] Mallat, S. (1999). *A Wavelet Tour of Signal Processing*. Academic, New York.

[35] C. Sidney Burrus Ramesh A. Gopnath Haitao Guo. (2008). *Introduction to wavelets and wavelet transforms: a primer*. Pearson Education Asia Limited and China Machine Press, Simplified Chinese edition, Beijing.

[36] Zieliński, T. (2004). Wavelet transform applications in instrumentation and measurement: tutorial and literature survey. *Metrol. Meas. Syst.*, 11(1), 61-101.

[37] Szmajda, M., Górecki, K., Mroczka, J. (2010). Gabor transform, spwvd, gabor-wigner transform and wavelet transform – tools for power quality monitoring. *Metrol. Meas. Syst.*, 17(3), 383-396.

[38] Barros, J., Diego, R.I. (2008). Analysis of harmonics in power systems using the wavelet-packet. *IEEE Trans. Instrum. Meas.*, 57(1), 63-69.

[39] Dwivedi, U.D., Singh, S.N. (2010). Enhanced Detection of Power-Quality Events Using Intra and Interscale Dependencies of Wavelet Coefficients. *IEEE Trans. Power Deliv.*, 25(1), 358-366.

[40] Moore, P.J., Carranza, R.D., Johns, A.T. (1994). A new numeric technique for high-speed evaluation of power system frequency. *IEE proc.-Gener. Transm. Distrib.*, 141(5), 529-536.

[41] Moore, P.J., Allmeling, J.H., Johns, A.T. (1996). Frequency relaying based on instantaneous frequency measurement. *IEEE Trans. Power Deliv.*, 11, 1737-1742.

[42] IEC 61000-4-7. (2002). Electromagnetic compatibility (EMC)—Part 4–7: Testing and Measurement Techniques, International Electrotechnical Commission.